

Speckle reduction of synthetic aperture imaging ladar based on wavelength characteristics

Qian Xu (许倩), Zhiwei Sun (孙志伟), Jianfeng Sun (孙建锋),
Yu Zhou (周煜)*, Zhiyong Lu (卢智勇), Xiaoping Ma (马小平), and Liren Liu (刘立人)

Key Laboratory of Space Laser Communication and Detection Technology, Shanghai Institute of Optics and Fine Mechanics, Chinese Academy of Sciences, Shanghai 201800, China

*Corresponding author: sunny@mail.siom.ac.cn

Received April 2, 2014; accepted April 29, 2014; posted online July 18, 2014

We propose a speckle-reduction method based on wavelength characteristics of speckle effect in synthetic aperture imaging ladar (SAIL). The return signal, which is the back scattering field with speckle effect from the rough surface of target, can be integrated over N chirp periods and heterodyne detected with a local-oscillator signal. After performing image processing respectively, the final image can be regarded as the incoherent superposition of the N sub-images. Numerical simulations indicate the effectiveness of this method. Our research may facilitate practical applications of SAIL.

OCIS codes: 030.6140, 280.6730, 280.3640, 110.3000.

doi: 10.3788/COL201412.080301.

Synthetic aperture imaging ladar (SAIL) can provide high imaging resolution because its laser source has higher frequency than radio wave^[1]. However, when coherent light is reflected from the rough surface of the target, a speckle pattern with a distinctive granular appearance is formed at receiving plane^[2]. Moreover, if linear frequency modulation signal is used, the speckle pattern in the scope of the optical antenna is temporally and spatially varied during SAIL data acquisition. Early studies have demonstrated that the speckle pattern shifts an average width in the range direction, which is equivalent to the scale of a footprint^[3]. As the ladar platform moves in the azimuth direction, random intensity and phase of the speckle are integrated by the optical receiving antenna aperture and the heterodyne detected with a local-oscillator (LO) signal. Thus, the phase of the heterodyne beat signal becomes time-varying instead of keeping constant. A time-dependent random phase is also imported to the quadratic phase history. Numerous institutes have obtained two-dimensional (2D) reconstructed images whose image quality has been reduced by laser speckle effect^[4–6].

Therefore, finding approaches to eliminate or at least reduce speckle effects is necessary. In a previous report^[7], multi-channel transmitting and receiving antenna systems are designed to decorrelate their respective speckles and reduce the non-uniformity of the return field. While these attempts are partially successful, the loss of spatial resolution and the requirement to significantly modify the imaging system hardware limit their practical application.

In this letter, we propose a speckle-reduction method based on the wavelength characteristics of the speckle effect in SAIL. Given that the SAIL speckle field distribution is related to the wavelength scan range, the return optical field with the random intensity and phase of speckle can be first integrated over N chirp periods and then heterodyne detected with a LO signal. After performing the image processing respectively, the final image can be regarded as the incoherent superposition

of the N sub-images.

Figure 1 shows the laser frequency chirping and the sampling of heterodyned signal^[8]. In a period of chirp pulse, the chirp is swept from the initial time t_0 to t_{end} , and the duration is $T_{\text{chirp}} = t_{\text{end}} - t_0$. Data collection begins at time t_{start} and ends at t_{stop} .

The sampling time is $T_f = t_{\text{stop}} - t_{\text{start}}$, and $\Delta\tau$ is the difference between the round-trip transit time of the target and the delay time of the LO. The initial frequency of optical pulse is f_{initial} and the end frequency is f_{final} . The bandwidth of heterodyne beat signal is $B = f_{\text{final}} - f_{\text{initial}}$ and the designed range resolution is $\rho_r = \frac{c}{2B}$, where c is the speed of light. Thus, the linear chirp rate can be written as $\dot{f} = \frac{c}{2T_f\rho_r}$. In practice, the linear modulation of the chirp laser is operated at the wavelength, not directly at the optical frequency. The chirped wavelength can be expressed as $\lambda(t_f) = \lambda_0 + \dot{\lambda}t_f$, where λ_0 is initial wavelength and $\dot{\lambda} = -\frac{\lambda^2}{c}\dot{f}$ is the wavelength linear chirp rate. The sweep bandwidth of the wavelength in a chirp pulse is $\Delta\lambda = \dot{\lambda}T_f = -\frac{\lambda^2}{2\rho_r}$. As indicated in a previous report^[3], the speckle pattern in the scope of an optical antenna is related to the operating wavelength $\lambda(t_f)$. The speckle pattern shifts to an average scale in the range direction as the chirped wavelength ranges from λ_0 to $\lambda_0 + \Delta\lambda$. Theoretically, the speckle granular distribution contains alternating dark and bright speckles, which can

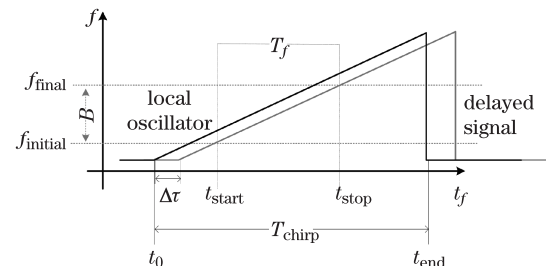


Fig. 1. Laser frequency chirping and sampling of heterodyned signal.

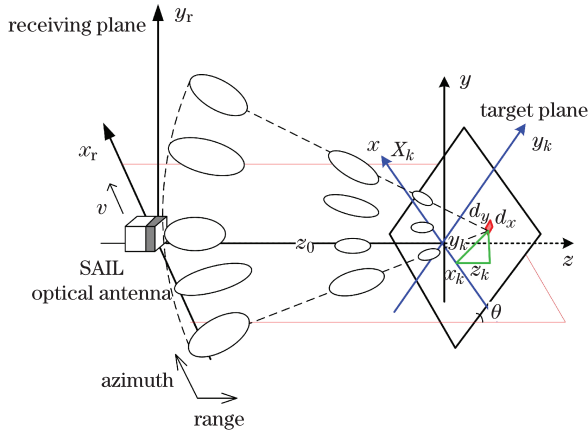


Fig. 2. (Color on line) Geometry for strip-mode SAIL speckle reception.

be characterized as pairs of speckle. They follow the same statistical theories, and are evenly distributed on the receiving plane.

In a typical SAIL system, x represents the azimuth direction and θ is the slope angle of the target plane. As depicted in Fig. 2, the coordinate system of the transmitting antenna of SAIL is (x_r, y_r) , the target coordinate system is (x_k, y_k) , and the scale of resolution element is $d_x \times d_y$. The range between SAIL and the center of the target plane is z_0 , and the range of the point (x_k, y_k) is $z = z_0 + y_k \cos \theta$. The velocity of SAIL along the azimuth direction is v . The optical aperture of the transmitting telescope is $L_x \times L_y$. For simplicity, the optical aperture of the receiving telescope is $L_x \times L_y$ as well. Fast time along the range direction is defined as t_f ($0 \leq t_f \leq T_f$). T_s is the interval between the transmitted pulses, and the discrete slow time in azimuth direction is $t_s = nT_s$. The average wavelength is λ . The resolution element can be divided into $M \times M$ pixels, and the coordinate of arbitrary pixel is $(x_k(i, j), y_k(i, j))$. The return speckle field in the scope of the receiving antenna can be expressed as a complex amplitude as^[3]

$$e_{\text{speckle}}(x_r, y_r; t_f, nT_s) = \frac{1}{M^2} \sum_{i \leq M, j \leq M} E(x_r, y_r; x_k(i, j), y_k(i, j)), \quad (1)$$

where $E(x_r, y_r; x_k(i, j), y_k(i, j))$ is the returning optical field of the (i, j) pixel, which can be written as

$$\begin{aligned} E(x_r, y_r; x_k(i, j), y_k(i, j)) &= \exp \left\{ j \frac{2\pi}{\lambda(t_f)} [z_0 + y_k(i, j) \cos \theta] \right\} \exp [j\varphi'(i, j)] \\ &\times \exp \left\{ j \frac{\pi}{\lambda(t_f) [z_0 + y_k(i, j) \cos \theta]} \left\{ [x_r - (x_k(i, j) - nvT_s)]^2 \right. \right. \\ &\left. \left. + (y_r - y_k(i, j) \sin \theta)^2 \right\} \right\}, \quad (2) \end{aligned}$$

where $\varphi'(i, j)$ is the random phase of the (i, j) pixel, which is imported by the rough target surface. The travelling receiving aperture can be written as

$$A(x_r, y_r; nT_s) = \text{rect} \left(\frac{x_r - vnT_s}{L_x} \right) \text{rect} \left(\frac{y_r}{L_y} \right). \quad (3)$$

Thus, the complex amplitude of the integrated speckle field over the receiving antenna aperture can be obtained as^[9]

$$S(x_r, y_r; t_f, nT_s) = \iint e_{\text{speckle}}(x_r, y_r; t_f, nT_s) * A(x_r, y_r; nT_s) dx_r dy_r, \quad (4)$$

which is a 2D distributed optical field related to the fast time t_f in the range direction and the slow time nT_s in the azimuth direction. The $*$ denotes a convolution. It represents the random intensity and phase distributions introduced by the speckle effect. After heterodyne detected with a LO signal, the heterodyne beat signal, which is needed to obtain the SAIL image, will be inevitably affected. The phase of heterodyne beat signal turns into time-varying instead of keeping constant, and a time-dependent random phase is also imported to quadratic phase history. Thus, the SAIL data collection equation with speckle effect from the target point (x_k, y_k) can be deduced by

$$\begin{aligned} I_{1D}(x_k, y_k; t_f, nT_s) &= K(x_k, y_k) \text{sinc} \left[\frac{(x_k - nvT_s)L_x}{\lambda z} \right] \\ &\text{sinc} \left(\frac{y_k L_y}{\lambda z} \right) S(x_k, y_k; t_f, nT_s) \times \text{rect} \left(\frac{t_f - T_f/2}{T_f} \right) \\ &\exp \left(j2\pi f t_f \frac{2\Delta z}{c} \right) \exp \left[j\pi \frac{(x_k - nvT_s)^2}{\lambda z} \right], \quad (5) \end{aligned}$$

which can be arranged in terms of a matrix of $m \times n$, where m is the row index in the range direction and n is the column index in the azimuth direction^[8]. In Eq. (5), $K(x_k, y_k)$ represents the receiving factor of optical field related with target reflectivity, SAIL structure, and system arrangement. The SAIL 2D data collection equation has the form

$$I_{2D}(x_k, y_k; t_f, t_s) = \sum_n I_{1D}(x_k, y_k; t_f, nT_s). \quad (6)$$

For an area distributive target, the return fields scattered from different resolution elements can be regarded as uncorrelated. Thus, the data acquisition of the area distributive target may be obtained

$$I_{2D}(x_T, y_T; t_f, t_s) = \sum_k I_{2D}(x_k, y_k; t_f, t_s). \quad (7)$$

Similarly, different resolution elements contribute a series of uncorrelated speckle patterns. These speckle patterns are statistically independent, as stated in Ref. [10], and summations on the complex amplitude basis have no effect on the form of the statistical characteristics. Thus the statistical characteristics of speckle effect introduced by the area distributive target are similar to the resolution element.

In order to mitigate the speckle effect of SAIL, we utilize the wavelength characteristics of the speckle effect. The wavelength linear chirp rate remains the same

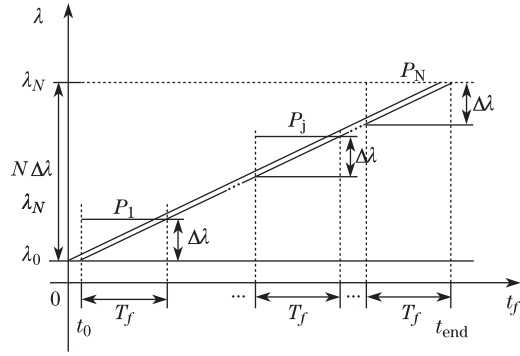


Fig. 3. Operating wavelength range will be extended to $N\Delta\lambda$.

and the sampling period can be increased $N(N \geq 2)$ times. As illustrated in Fig. 3, the operating wavelength range will be extended to $N\Delta\lambda$ and the shift length of speckle in the range direction will be equal to N times of the speckle average width. Moreover, the collected data will be extended to a matrix of $N * m \times n$, which is composed of N submatrices. The size of each submatrix is $m \times n$. The wavelength of the j th ($1 \leq j \leq N$) submatrix is swept from $\lambda_{j-1} = \lambda_0 + (j-1) \cdot \Delta\lambda$ to $\lambda_j = \lambda_0 + j \cdot \Delta\lambda$.

The earlier subsections demonstrate that both intensity and phase distributions of the integrated speckle field over the receiving antenna aperture are characterized with the chirped wavelength range, and their influences on SAIL imaging are significantly different. The N submatrices are performed the image processing respectively, and then the N sub-images are obtained. Given that the 2D data are first compressed by Fourier transform in the range direction, and match filtering algorithm is adopted to achieve the image in the azimuth direction^[11], the j th sub-image can be expressed as

$$I_j(x_k, \Delta z) = K_j(x_k, y_k) \left[S_{\text{range},j}(\xi) * \delta\left(\xi - j\frac{2\Delta z}{c}\right) \right] [S_{\text{azimuth},j}(nvT_s) * \delta(nvT_s - x_k)]. \quad (8)$$

The coordinates of the image are given by $\Delta z = c\xi/2\dot{f}$ and $x_k = nvT_s$. $S_{\text{range},j}(\xi)$ and $S_{\text{azimuth},j}(nvT_s)$ are the j th impulse responses respectively in the range and azimuth directions. The final image can be regarded as the incoherent superposition of the N sub-images, which can be approximately expressed as

$$\begin{aligned} I(x_k, \Delta z) &= \frac{1}{N} \sum_{j=1}^N |I_j(x_k, \Delta z)| \\ &= \frac{1}{N} \sum_{j=1}^N K_j(x_k, y_k) \left| S_{\text{range},j}(\xi) * \delta\left(\xi - j\frac{2\Delta z}{c}\right) \right| \\ &|S_{\text{azimuth},j}(nvT_s) * \delta(nvT_s - x_k)|. \end{aligned} \quad (9)$$

Moreover, the average intensity and root-mean-square (rms) contrast of the image are proposed to quantify the degree to which speckle reduces the image quality. For the j th sub-image, the average intensity is

$$\mu_j = \frac{1}{m \times n} \sum_{r=1}^m \sum_{a=1}^n I_{r,a}, \quad (10)$$

where $m \times n$ is the total number of pixels in the imaging region and $I_{r,a}$ is the intensity of each pixel. The rms contrast^[12] of the j th sub-image can be defined as

$$\text{rms}_j = \left[\frac{1}{m \times n - 1} \sum_{r=1}^m \sum_{a=1}^n (I_{r,a} - \mu_j)^2 \right]^{1/2}. \quad (11)$$

Thus the average intensity of the final image can be written as

$$\mu_I = \frac{\mu_1 + \mu_2 + \dots + \mu_N}{N}, \quad (12)$$

and therns contrast is

$$\text{rms}_I = \left[\frac{1}{N \cdot (m \times n) - 1} \sum_{j=1}^N \sum_{r=1}^m \sum_{a=1}^n (I_{r,a;j} - \mu_I)^2 \right]^{1/2}. \quad (13)$$

Statistically, when the sampling periods number N is very large, the amplitude of the integrated speckle fields over the receiving antenna aperture obeys Rayleigh statistics and the phase is uniformly distributed on the $(-\pi, \pi)$ ^[10]. Thus, after image processing and incoherent superposition of the N sub-images, the influences of the N integrated speckle fields can be mitigated and the quality of the SAIL image is improved.

Based on the model of the strip-mode airborne SAIL, the parameter settings of the numerical simulation are given in Table 1.

Here we characterize the multiple of the sampling period as $N = 2$ to simulate the effectiveness of this speckle-resistant method. For the first subpulse, the operating wavelength scans from $\lambda_0 = 1550.5149$ nm to $\lambda_1 = 1550.5829$ nm. The 2D distribution of the integrated speckle field over the receiving antenna aperture is shown in Fig. 4. Figure 4(a) depicts the amplitude distribution. The average value of the amplitude is 4.1639×10^4 , and the standard deviation value is 6.6635×10^3 . Figure 4(b) depicts the phase distribution. The average value of the phase is 0.1193 rad, and the standard deviation value is 0.3242 rad.

Table 1. Strip-mode Airborne SAIL Parameter Settings

Parameter	Value
Velocity of Platform (v)	50 m/s
Speed of Light (c)	3.0×10^8 m/s
Observation Angle (θ)	45°
Slant Range (z_0)	15 km
Transmitting Aperture ($L_x \times L_y$)	0.05×0.05 (m)
Receiving Aperture ($D_x \times D_y$)	0.05×0.05 (m)
Designed Resolution ($d_x \times d_y$)	2.5×2.5 (cm)
Footprint Diameter (D_{fp})	0.93 m
Pulse Initial Wavelength (λ_0)	1550.5149 nm
Transmitted Pulse Interval (T_s)	0.5 ms
Pulse Duration Time (t_f)	0.1 ms
Chirp Bandwidth (B)	8.49×10^9 Hz
Frequency Chirp Rate (\dot{f})	8.49×10^{13} Hz/s
Wavelength Scan Rate ($\dot{\lambda}$)	680 nm/s
Wavelength Scan Range ($\Delta\lambda$)	0.068 nm

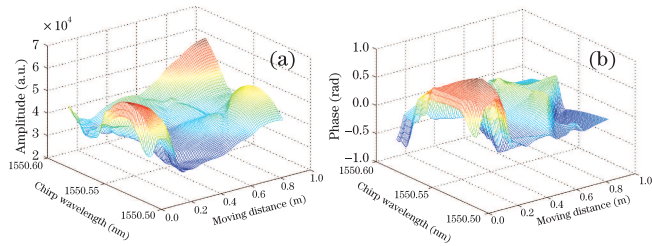


Fig. 4. (a) Amplitude and (b) phase distribution of the integrated speckle field over the receiving antenna when $\lambda(t_f) = 1550.5149 - 1550.5829$ nm.

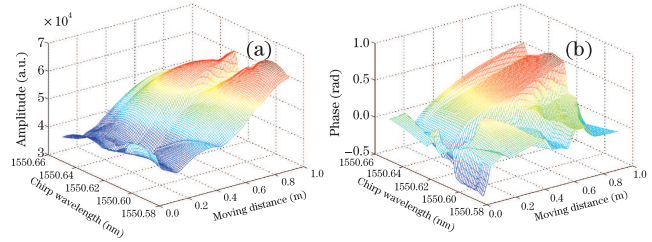


Fig. 5. (a) Amplitude and (b) phase distribution of the integrated speckle field over receiving antenna $\lambda(t_f) = 1550.5829 - 1550.6509$ nm.

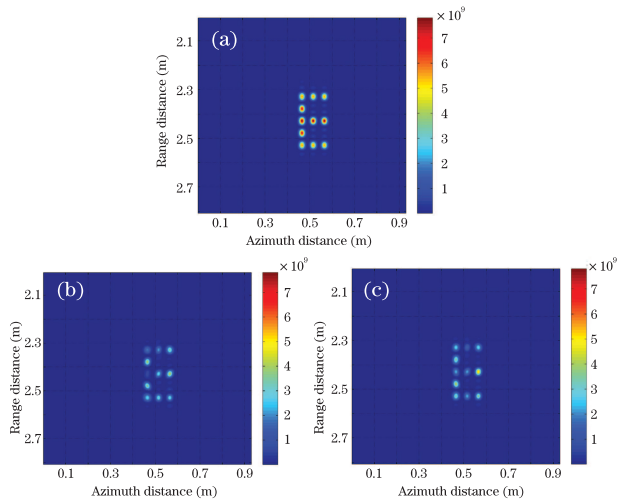


Fig. 6. (a) Ideal, (b) speckle affected, and (c) speckle mitigated images of the simulated target “E”.

The wavelength scanning range for the second subpulse is from $\lambda_1 = 1550.5829$ nm to $\lambda_2 = 1550.6509$ nm. Figure 5(a) shows the amplitude distribution of the integrated speckle field, and Fig. 5(b) shows the phase distribution. The average value of the amplitude is 4.9245×10^4 , and the standard deviation value is 7.4352×10^3 . Meanwhile, the average value of the phase is 0.1328 rad, and the standard deviation value is 0.2034 rad.

Apparently, the integrated speckle amplitude and phase distribution are related to the wavelength scan range. We assume a letter “E” as the simulated target, with a slant angle of 45° from the horizontal plane. It is composed of five resolution elements in the range direction and three elements in the azimuth direction. The resolution element scale is designed as $d_x \times d_y = 2.5 \times 2.5$ (cm), and the interval between neighboring resolution elements is 5 cm. Correspondingly, the region of the target is approximately from 2.20 to 2.60 m in the range direction and 0.42 to 0.62 m in the azimuth

direction. Figure 6(a) shows the ideal image of the target, which has the maximum intensity of 7.8098×10^9 . According to Eqs. (12) and (13), the average image intensity of the ideal image is 5.5610×10^8 , and the value of the contrast is 1.2610×10^9 .

Figure 6(b) shows the image affected by the speckle when the wavelength scan range is from $\lambda_0 = 1550.5149$ nm to $\lambda_1 = 1550.5829$ nm. The maximum intensity is 4.1815×10^9 . The value of the average image intensity is decreased to 2.6987×10^8 , about half of the ideal image, indicating that the speckle effect leads to the reduction of image intensity. The value of the contrast declines to 5.8396×10^8 , so the speckle effect leads to the reduction of the image contrast in SAIL.

Figure 6(c) illustrates the image after the speckle effect is mitigated. Compared with Fig. 6(b), the maximum intensity is 5.2710×10^9 , the value of the average image intensity rises to 2.8388×10^8 , and the value of the contrast is increased to 6.2715×10^8 . Simulation results indicate that both the average intensity and the image contrast are increased after using the speckle-resistant method. Thus the method using wavelength characteristics is effective to reduce the influence of speckle effect on the SAIL image quality.

In conclusion, we propose a new speckle-reduction method based on the wavelength characteristics of the speckle effect to reduce the influence on the SAIL image quality. Given that the integrated speckle field over the receiving antenna aperture is related to the wavelength scan range, so the return optical field with the speckle effect can be integrated over N chirp periods and then heterodyne detected with a LO signal. The N sub-images of neighboring chirped wavelength are incoherent superposed to obtain the final image. Furthermore, we simulate a typical example when the multiple of the sampling period $N = 2$. The simulation results show that the average intensity and the contrast of the SAIL image are improved, which indicates the effectiveness of this method. Further numerical calculation and the specific relation between the quality of the SAIL image and sampling period number will be studied in the future. This research may facilitate practical applications of speckle effect suppression in SAIL.

This work was supported by the National Natural Science Foundation of China under Grant Nos. 61377004, 61108069, and 61275110.

References

1. S. M. Beck, J. R. Buck, W. F. Buell, R. P. Dickinson, D. A. Kozlowski, N. J. Marechal, and T. J. Wright, *Appl. Opt.* **44**, 7621 (2005).
2. J. C. Dainty, *Laser Speckle and Related Phenomena* (Springer-Verlag, New York, 1984).
3. Q. Xu, Y. Zhou, J. Sun, Z. Sun, X. Ma, Y. Zhi, and L. Liu, *Acta Opt. Sin.* **33**, 1028002 (2013).
4. M. Bashkansky, R. L. Lucke, E. Funk, L. J. Rickard, and J. Reintjes, *Opt. Lett.* **27**, 1983 (2002).
5. Y. Zhou, N. Xu, Z. Luan, A. Yan, L. Wang, J. Sun, and L. Liu, *Acta Opt. Sin.* **29**, 2030 (2009).
6. Y. Yan, J. Sun, X. Jin, Y. Zhou, Y. Zhi, and L. Liu, *Chin. Opt. Lett.* **10**, 091101 (2012).
7. L. Liu, *Acta Opt. Sin.* **31**, 1028001 (2011).

8. L. Liu, Acta Opt. Sin. **29**, 1408 (2009).
9. Q. Xu, Y. Zhou, J. Sun, Z. Sun, X. Ma, Y. Zhi, and L. Liu, Acta Opt. Sin. **34**, 0328002 (2014).
10. J. W. Goodman, *Speckle Phenomena in Optics: Theory and Applications* (Ben Roberts & Company, New York, 2007).
11. L. Liu, Appl. Opt. **52**, 579 (2013).
12. E. Peli, J. Opt. Soc. Am. A. **7**, 2032 (1990).